Composites: Part B 43 (2012) 819–824

Contents lists available at ScienceDirect

Composites: Part B

journal homepage: www.elsevier.com/locate/compositesb

Numerical simulations for class A surface finish in resin transfer moulding process

Geneviève Palardy [a], Pascal Hubert [a,*], Eduardo Ruiz [b], Mohsan Haider [a], Larry Lessard [a]

[a] Department of Mechanical Engineering, McGill University, 817 Sherbrooke Street West, Montreal, QC, Canada H3A 2K6
[b] Département de Génie Mécanique, Ecole Polytechnique de Montréal, C.P. 6079, succ. Centre-Ville, Montréal, QC, Canada H3C 3A7

ARTICLE INFO

Article history:
Received 1 June 2010
Received in revised form 27 May 2011
Accepted 1 June 2011
Available online 24 June 2011

Keywords:
A. Polymer–matrix composites
B. Surface properties
C. Analytical modeling
E. Resin transfer moulding

ABSTRACT

Simulation tools for Liquid Composite Moulding (LCM) processes are a key to predict and solve manufacturing issues. Despite the fact that numerical process analyses are commonly used to predict mould filling, resin cure and exothermic temperatures, more comprehensive computational tools are still required. Resin additives such as low profile additives (LPA) show a significant impact on process performance and part quality. In this work, mould pre-heating experiments were compared to numerical predictions using commercial simulation software. Non-isothermal simulations were then carried out and the predicted flow and degree-of-cure evolution were compared to experiments. Finally, a volume change model, previously developed, was implemented in this work to calculate mould pressure increases in RTM of resins with four different LPA contents (0%, 5%, 10% and 40%). The predictions were compared to the results from the mould pressure transducers in the mould cavity. Simulation results matched closely with the experimental results. Pressure evolution of low profile resins was found to be very sensitive to the model parameters.

1. Introduction

Potential benefits of advanced composite materials include reduced weight, superior stiffness/strength, increased corrosion resistance and good design flexibility. Liquid Composite Moulding (LCM) manufacturing techniques, which include resin transfer moulding (RTM), are attractive to the automotive industry because of low cost, good mechanical performance and part reproducibility. However, there are several process-related issues associated with the use of these manufacturing techniques. Improper mould filling because of inadequate mould design can result in dry spots, void formation and poor surface quality. Lack of knowledge about cure kinetics results in longer cycle times, higher manufacturing costs and poor part quality. Numerical simulations of LCM processes, which can predict mould pre-heating, cavity filling and resin curing during isothermal and non-isothermal cycles, have great potential to reduce costs and even eliminate process related problems.

RTM process simulation issues have been addressed by many researchers. Computer models simulating the resin flow front progression inside 2D RTM moulds were developed in [1–3]. Based on this work, many researchers have investigated mould filling and pressure distribution under isothermal or non-isothermal conditions for complex geometries, including 2D and 3D [4]. A numerical code that predicts the flow pattern in anisotropic media was developed in [5] where the effect of anisotropic preforms, inserts and mould thickness on the flow pattern was investigated. Numerical simulation of 3D mould filling in RTM was carried out through quasi-steady state and partial saturation formulations in [6]. Numerical schemes were evaluated by comparison with analytical solutions for simple geometries and good agreement was observed. A semi-empirical model was suggested for macro and micro impregnation of fibres during filling based on Darcy's law and capillary effects [7].

The effect of stacking sequence of the fibre mat and inlet pressure on the flow front position and its comparison with experimental results was investigated with 2D and 3D numerical models [8]. However, imperfections were observed for thick parts. This research also established the relationship between position of injection port and vent port with flow fronts and maximum pressures observed during injection. Models were also developed to determine optimum gate location and predict filling time for the RTM process [9–11].

PAM-RTM is a numerical code based on non-conforming finite element methods [12,13]. This code was used to study the position of flow front through multi-layer fibre reinforcement for 3D isothermal flow and reasonable agreement was obtained with experimental results [14]. Recent efforts in the area of RTM simulations include prediction of edge effects and heat conduction from the mould wall [15,16]. Mathematical modeling and numerical simulation of the RTM process cycle was carried using a Lagrangian formulation and saturation functions where the preform was modeled as a deformable porous solid [17]. The code was found to be very effective in predicting injection time, injection pressure and residual strains in

* Corresponding author.
E-mail address: pascal.hubert@mcgill.ca (P. Hubert).

1359-8368/$ - see front matter © 2011 Elsevier Ltd. All rights reserved.
doi:10.1016/j.compositesb.2011.06.002

the preform. A review of RTM modeling and simulation approaches taken from the literature is presented in [18].

Despite the large amount of existing work in the area of LCM numerical simulations, there is need for more detail-oriented studies and development of computational tools for the RTM process since a comprehensive and complete numerical simulation software is still absent. Advancements in resin technology and particularly the introduction of resins with low profile additives (LPA) have strengthened this need. LPA are thermoplastic additives that compensate for resin shrinkage by phase separation and micro-void formation. This mechanism is reported in detail elsewhere [19]. The development of mathematical and numerical tools to predict shrinkage–expansion behaviour of these resin systems during curing and their integration with already existing numerical codes has become an essential objective for RTM. There is also a need to validate already existing numerical codes with experimental data for the mould pre-heating, filling and curing stages. Unfortunately, the behaviour of low profile resins is not well understood and models to predict low profile resin behaviour are non-existent.

The purpose of this study is to incorporate mathematical models into already existing software to simulate LPA behaviour during actual manufacturing. In this paper, PAM-RTM software was used to study the pre-heating behaviour of a steel RTM mould. Simulated and experimental results were compared to validate the numerical predictions. Variations in degree-of-cure and pressure during the cure cycle were studied during non-isothermal processing. Finally, volume change models developed in a previous work [19] to predict the low profile resin shrinkage–expansion behaviour during cure were incorporated into the software to predict pressure variations caused by LPA. A comparison was carried out between measured and predicted mould pressure variations during the cure of resins with four different LPA contents: 0%, 5%, 10% and 40%.

2. Experimental

Composite plates were manufactured using a heated steel mould mounted on a hydraulic press. The mould had a mirror-like polished finish and was instrumented with type J thermocouples and Dynisco PT422 pressure sensors connected to a Vishay 6000 data acquisition system. The mould platens were heated to the required temperatures with a Conair circulating water heating system. The resin at room temperature was injected into the mould cavity with a Radius Engineering constant pressure pneumatic-controlled injector. The 3.175 mm thick picture frame was sealed using a Gore-Tex joint sealant gasket. A temperature gradient was created by setting the top and bottom platens at two different temperatures (in a range from 75 °C to 90 °C). The bottom mould was always kept at 90 °C whereas the temperature of the top one was adjusted to achieve the required gradient. The 24 cm by 26 cm F3P glass fibre preform was cut and placed inside the mould just before injection. Side-A of the preform was turned towards the hottest mould platen. The pressure sensors (referred to as PS1, PS2, PS3 and PS5) were located near the injection and vent ports and PS4 was mounted on the pump to measure injection pressure. The injections were performed at different pressure levels ranging from 200 to 650 kPa. Manufactured composite panels were kept inside the mould until the resin achieved the maximum pressure level (20–30 min). A schematic of the fibre preform is given in Fig. 1. Resin tracers were used to verify the uniformity of the flow front.

2.1. Material properties

The RTM mould used in this work was made of 1.5% carbon steel. Scott Bader's PD9551 polyester resin with and without LPA (0%, 5%, 10% and 40% by weight) was used for RTM manufacturing. A glass fibre mat preform was used for which permeabilities were measured in a previous work [20]. The mould, resin and fibre perform properties used in the computational analysis are given in Table 1. A cure kinetic model was adapted from Kamal–Sourour's model for a low profile polyester resin [19]. The corresponding model is given in the following equation:

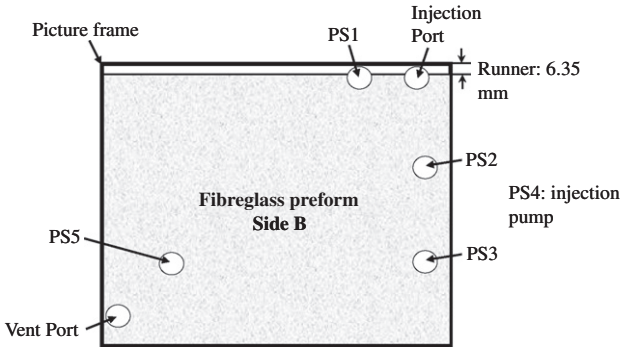

Fig. 1. Position of the pressure sensors on the composite panel, PS4 is on the injection pump.

Table 1
Thermal and transport properties of the materials used for the simulations.

Property	Mould	Resin	Fibre preform
Density (kg/m^3)	6850	1260	2500
Specific heat (J/kg K)	500	1600	700
Thermal conductivity (W/m K)	36	0.25	0.1
Reaction enthalpy (kJ/kg)	–	400	–
Permeability (m^2)	–	–	4.163×10^{-10}

$$\frac{d\alpha}{dt} = (K_1 + K_2\alpha^m)(\alpha_{max} - \alpha)^n$$
$$K_i = A_i \exp\left(-\frac{E_i}{RT}\right) \quad i = 1,2 \tag{1}$$

where α is the degree-of-cure, α_{max} is maximum degree-of-cure achieved in an isothermal scan ($\alpha_{max} = 0.9$), R is ideal gas constant, T is temperature, E_1 and E_2 are activation energies ($E_1 = 149.7$ kJ mol^{-1}, $E_2 = 87.54$ kJ mol^{-1}), A_1 and A_2 are Arrhenius constants ($A_1 = 1.07 \times 10^{13}$ s^{-1}, $A_2 = 7.20 \times 10^{10}$ s^{-1}) and m and n are kinetic exponents ($m = 0.711$, $n = 1.464$). Castro and Macosco's viscosity model combined with Arrhenius' law (Eq. (2)) was also used in simulations to predict changes in resin viscosity during filling and curing.

$$\eta(\alpha, T) = \eta_O(T)\left(\frac{\alpha_G}{\alpha_G - \alpha}\right)^{(C_1 + C_2\alpha)}$$
$$\text{where} \quad \eta_O(T) = B\exp\left(\frac{T_b}{T}\right) \tag{2}$$

where $\eta_O(T)$ is the viscosity at a given temperature, T is temperature in Kelvin, α is degree-of-cure, α_G is degree-of-cure at gelation ($\alpha_G = 0.055$) and T_b, B, C_1 and C_2 are model parameters obtained from linear regression techniques ($T_b = 2701$°K, $B = 1.51 \times 10^{-4}$ Pa s. $C_1 = 1.502$, $C_2 = 1.010$). The shrinkage of the neat polyester resin (0% LPA) was also measured through a procedure presented in [19]. Eq. (3) predicts the resin shrinkage behaviour as a function of degree-of-cure.

Table 2
Parameters for LPA shrinkage–expansion model (Eqs. (3)–(6)).

$\left(\frac{\Delta V}{V}\right)_{Shrinkage}$ Eq. (3)					
Parameters	α_G 0.05	α_M 0.8	$(\Delta V/V)_{Total}$		
Values	5	98	9.186		
$\left(\frac{\Delta V}{V}\right)_{LPA}$ Eq. (5)					
Parameters	α_C	α_F			
Values	0.320	0.898			
$\left(\frac{\Delta V}{V}\right)_{TEX}$ Eq. (6)					
Parameters	c_1	c_2	X_c	X_M	X_F
Values	−12.126	0.115	6.844	10.08	40

$$\begin{aligned}\left(\frac{\Delta V}{V}\right)_{Shrinkage} &= 0 < \alpha \leqslant \alpha_G \\ \left(\frac{\Delta V}{V}\right)_{Shrinkage} &= \left(\frac{\alpha-\alpha_G}{\alpha_M-\alpha_G}\right)\left(\frac{\Delta V}{V}\right)_{Total} \quad \alpha_G < \alpha < \alpha_M \\ \left(\frac{\Delta V}{V}\right)_{Shrinkage} &= \left(\frac{\Delta V}{V}\right)_{Total} \quad \alpha \geqslant \alpha_M\end{aligned} \tag{3}$$

where α is resin degree-of-cure, α_G is degree-of-cure at gelation and α_M is degree-of-cure corresponding to the total cure shrinkage. For the neat resin α_G is 0.055, α_M is 0.898 and $(\Delta V/V)_{Total}$ is 9.186%.

A specific amount of LPA is needed to compensate the chemical shrinkage of the resin [19]. The shrinkage–expansion behaviour of low profile resin was modeled using rheological techniques. The model of combined shrinkage-LPA action is given by Eqs. (4)–(6). This model adequately predicts the shrinkage and expansion behaviour of a low profile resin as a function of degree-of-cure. Its parameters, obtained from experimental values, are listed in Table 2.

$$\left(\frac{\Delta V}{V}\right)_{Total} = \left(\frac{\Delta V}{V}\right)_{Shrinkage} + \left(\frac{\Delta V}{V}\right)_{LPA} \tag{4}$$

where $\left(\frac{\Delta V}{V}\right)_{Shrinkage}$ is obtained from Eq. (3) and $\left(\frac{\Delta V}{V}\right)_{LPA}$ is given by:

$$\begin{aligned}\left(\frac{\Delta V}{V}\right)_{LPA} &= 0 < \alpha \leqslant \alpha_C \\ \left(\frac{\Delta V}{V}\right)_{LPA} &= \left(\frac{\alpha-\alpha_C}{\alpha_F-\alpha_C}\right)\left(\frac{\Delta V}{V}\right)_{TEX} \quad \alpha_C < \alpha \leqslant \alpha_F \\ \left(\frac{\Delta V}{V}\right)_{LPA} &= \left(\frac{\Delta V}{V}\right)_{TEX} \quad \alpha > \alpha_F\end{aligned} \tag{5}$$

where $\alpha_C = 0.32$, $\alpha_F = 0.898$ and $\left(\frac{\Delta V}{V}\right)_{TEX}$ corresponds to LPA expansion and is a function of LPA content (X_{LPA}) as:

$$\begin{aligned}\left(\frac{\Delta V}{V}\right)_{TEX} &= 0 \quad \text{for} \quad X_{LPA} \leqslant X_c \\ \left(\frac{\Delta V}{V}\right)_{TEX} &= c_1\left(\frac{X_{LPA}-X_c}{X_M-X_c}\right) \quad \text{for} X_c < X_{LPA} \leqslant X_M \\ \left(\frac{\Delta V}{V}\right)_{TEX} &= c_2(X_{LPA}-X_M)+c_1 \quad \text{for} X_M < X_{LPA} \leqslant X_F\end{aligned} \tag{6}$$

where $X_c = 6.844\%$, $X_M = 10.08\%$, $X_F = 40\%$, $c_1 = -12.126$ and $c_2 = 0.115$.α_C is the degree-of-cure of low profile resin where shrinkage stops and expansion starts.

3. Results and analysis

A detailed 3D CAD model was created with I-DEAS to the same dimensions as that of the actual mould. The water channels were set at the experimental temperature for each mould platen. A forced convective heat transfer coefficient of 12,455 W/m^2°C was used for heating channels. This coefficient was calculated based on the flow rate and diameter of the channels with the Dittus–Boelter correlation. A free convective heat transfer coefficient of 7 W/m^2°C was used for all the nodes in contact with free air. Four thermocouples were placed in the experimental set-up in order to follow the temperature gradients. Pre-heating simulations were carried out under identical boundary conditions. The temperature evolution was almost identical for the sensors on both mould platens, which means that temperature evolution depended only on the location of the sensor irrespective of the isothermal temperature level.

3.1. Non-isothermal filling simulations

A non-isothermal filling simulation was carried out for a rectangular picture frame (Fig. 1). The resin runner (with a width of 6.35 mm) was designed to obtain a linear resin flow through the fibres. Non-isothermal injections were done under constant injection pressures (in a range between 200 and 650 kPa). A temperature gradient of 10 °C was also considered between the top and bottom mould platens. Material properties listed in Section 2.1 were used for filling and curing simulations. In the experimental set-up, coloured tracers were applied on the preform to monitor the resin flow evolution during injection. A straight line flow pattern was observed on all the samples. The simulated resin flow during a non-isothermal injection at a pressure of 345 kPa moved in a linear fashion. The flow front was found to be a straight line for low injection pressures.

Filling simulations were carried out for other injection pressure levels and injection times were predicted. An error of less than 10% was found between the predicted and experimentally measured filling times. The injection time decreased (from 50 to 10 s) with increasing injection pressures (from 200 to 650 kPa). In Fig. 2, a comparison between experimental and numerical pressure evolutions is presented for an injection pressure of 345 kPa. A close match between measured and predicted values can be observed at the three positions along the mould cavity (PS1, PS2 and PS3). PS1 and PS2, closer to the injection port, increase gradually, whereas PS3, closer to vent port, increases sharply. No pressure is read by the sensors until the flow front reaches their location. Shortly after the flow front reaches PS3, it flows out of the vent port. The vent port is then closed and a sharp increase in pressure can be observed on the sensor locations. The simulation software therefore gave a satisfactory prediction of the pressure increase during RTM manufacturing.

3.2. Curing simulations

In the selected manufacturing process, the temperature gradient between the upper and lower mould platens induces a curing gradi-

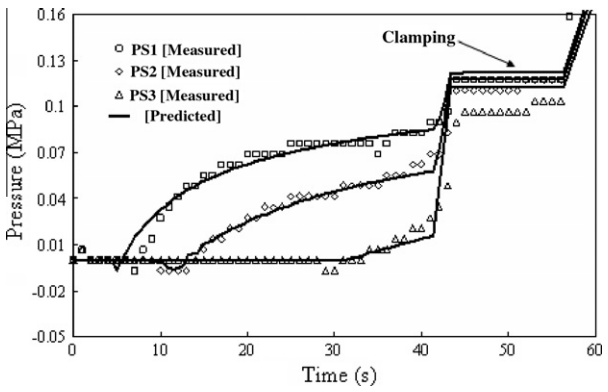

Fig. 2. Pressure variation at sensor locations shown in Fig. 1 during injection: measure and simulated results.

ent through the part thickness. In Fig. 3, the simulated resin degree of cure is plotted at three positions through the thickness of the mould cavity (i.e. top surface, part core and bottom surface) closer to the vent port. The surface of the part that is adjacent to the hottest mould platen starts to cure first and a through-thickness cure gradient is observed. Due to the temperature differences between the mould and the resin prior to injection, the cure gradient is not only observed through the thickness, but also along the length of the part. Non-isothermal filling and curing analyses were carried out to simulate the curing process on the test plate. A cure gradient can be observed between the vent gate and the injection port. This phenomenon is plotted in Fig. 4 for PS1 and PS5. The resin at PS5, which is close to the vent port, starts curing first, followed by the resin further away from the vent port. There is a time lag of approximately 1 min between the curves for the two locations. However, if the time difference between the two curves is removed, they fall perfectly onto each other. This in-plane cure gradient can also be experimentally verified by the pressure drops along the part surface (see Fig. 5). Initially, a constant pressure level is seen at all sensor locations because of the hydrostatic pressure when the mould vents are clamped at the end of injection. A pressure drop is then observed at the sensor because of the resin gelation and shrinkage. However, the pressure drop at those locations does not occur at the same time, which is due to the cure gradient along the part. The sensors closer to the vent port (PS3 and PS5) show that gelation and shrinkage happen earlier compared with the sensors closer to the injection port. A time lag of approximately 1 min is present between PS5 and PS1, which is consistent with the degree-of-cure evolution lag presented in Fig. 4.

3.3. Pressure simulations

It was observed that low profile resins shrink at the beginning and expand at the later stage of the cure cycle [19]. The resin expansion during polymerisation causes an increase of the mould

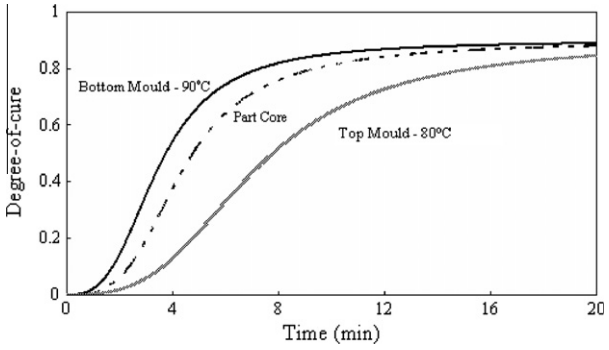

Fig. 3. Through thickness degree-of-cure variations (on the top, bottom and middle of the part) close to the vent port when manufactured with a temperature gradient of 10 °C.

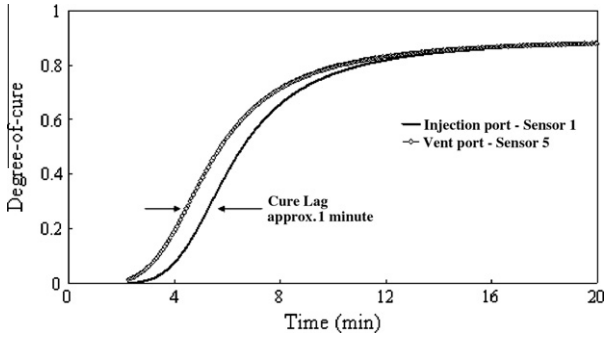

Fig. 4. Cure gradient between the injection and vent ports.

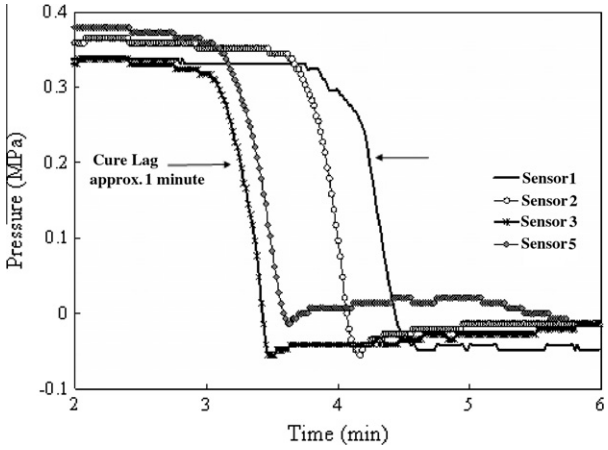

Fig. 5. Pressure drop at different sensor locations representing the in-plane cure gradients and gelation of a polyester resin (sensor locations shown in Fig. 1).

pressure [20]. During the cure of LPA resins, mould pressure indicates an intimate contact between the part and the mould surface. This wall-to-wall contact guaranties a good surface finish of the composite part. Hence, the monitoring of the mould pressure is important to achieve successful moulding conditions for class A surface finish. In this work, a numerical model was developed to predict the pressure variations during the cure of LPA resins. Based on Rudd et al. [21], the mould pressure (M_p) can be calculated by the following equation:

$$Mp = \Delta V \cdot \left(E_m + \frac{1}{\frac{\phi}{E_r} + \frac{1-\phi}{G_f}} \right)(1 + v_r) + Hp \tag{7}$$

where ΔV is the total volume change of the composite part (i.e. thermal and chemical volume changes). E_m is initial resin elastic modulus ($E_m = 8.73 \times 10^7$ Pa). E_r is resin elastic modulus that evolves during cure. G_f is shear modulus of the fibres. v_r is Poisson's ratio of the composite. φ is the porosity of the reinforcement ($\varphi = 0.8$). Hp is initial hydrostatic pressure (i.e. the pressure at the end of injection, $H_p = 250$ kPa).

ΔV, E_r, G_f, and v_r, are functions of degree-of-cure. The evolution of E_r, G_f, and v_r during cure is discussed in detail by Ruiz and Trochu [22]. The volume change (ΔV) during cure was characterised for different LPA resin systems in [20] (0%, 5%, 10% and 40% LPA). Two sources were identified for the volume changes: thermal expansion/contraction and chemical shrinkage/expansion. However, it was shown that the resin injected in the mould cavity reached a constant temperature after approximately 30 s [20]. Therefore, the model of volume change during cure only considers the effect of chemical shrinkage/expansion. For a neat polyester resin, ΔV is given by Eq. (3) and for an LPA-based resin, is given by Eq. (4). The models are plotted in Fig. 6 along with the experimental data calculated from rheology and DSC experiments. Eq. (7) was then solved at each time step during the curing simulation to calculate the mould pressure using the volume change model of Eqs. (3)–(6). Since the predicted degree-of-cure evolution varies within the part thickness, it was taken at the part core, as seen in Fig. 7 shows a comparison between the measured and numerically predicted pressures at PS1 (near the injection port). While the predictions are close to the measured values, there is a small inaccuracy in the time at which pressure starts to increase for 10% and 40% LPA (2 min difference). It suggests that the model predicts that the LPA expansion occurs later than it does during the experiments. To understand how the model parameters influence the predicted pressure curve, α_c and c_1 were varied while keeping

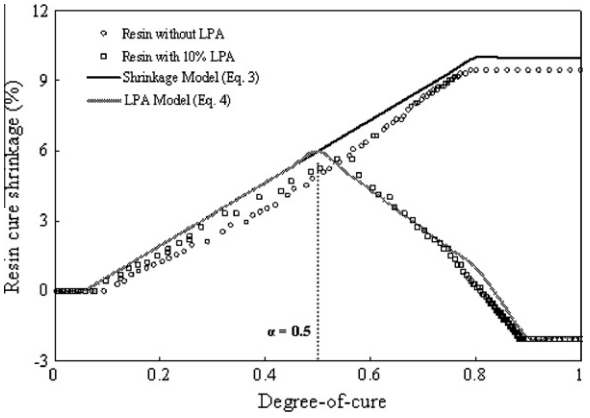

Fig. 6. Volume change during cure of a resin with and without LPA (a) chemical shrinkage below $\alpha < 0.5$ and (b) chemical expansion (LPA compensation) above $\alpha > 0.5$.

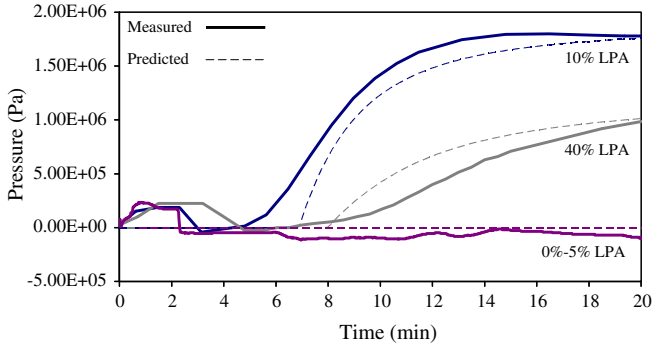

Fig. 7. Measured and predicted pressure evolutions for during the cure of resin systems with four different LPA contents (0%, 5%, 10% and 40%).

the total volumetric shrinkage at 9.186% (Table 2). Those two parameters were chosen because it was observed in Fig. 6 that they were the only ones that had a significant effect on the onset of LPA expansion, the maximum cure shrinkage and the final shrinkage or expansion value. Results were plotted in Figs. 8 and 9 for a standard resin system with 10% LPA. A total of three values for α_c were chosen based on the original model value: 0.35 ± 0.10. Fig. 8 shows that when α_c decreases by 0.10, the time at which the LPA expansion occurs decreases by approximately 1 min. Three values of c_1 were chosen: −11.0, −12.126 (original value from the model) and −13.0. Fig. 9 shows that this parameter has an effect on the onset of LPA expansion and the final pressure. When c_1 increases, the onset of LPA expansion decreases while the final pressure increases. For both parameters, it was seen that small changes translate into relatively large variations in the predicted pressure. The discrepancies in Fig. 7 may be attributed to such parameters variations as the model was based on experimental data (Fig. 6).

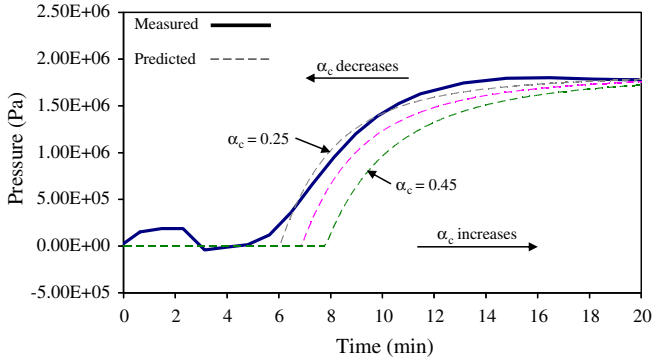

Fig. 8. Pressure predictions for various α_c (0.25, 0.35 and 0.45) for a resin system with 10% LPA.

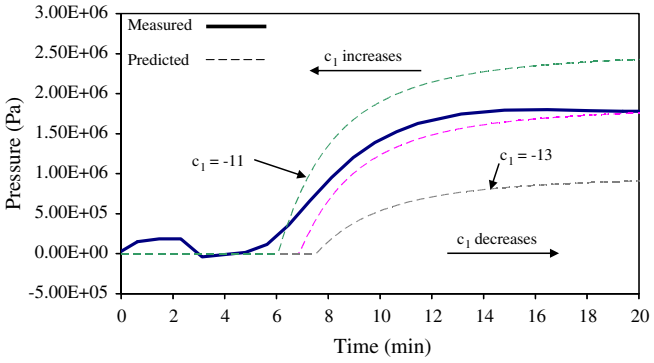

Fig. 9. Pressure predictions for various c_1 values (−11.0, −12.126 and −13.0) for a resin system with 10% LPA.

4. Conclusion

Mould pre-heating, filling, curing and pressure-variation simulations closely matched with the experimental results. Flow patterns made by marked tracers on the surface of the preform followed closely the filling simulations. These results were further confirmed by the similarity between measured and predicted filling times and pressure variations observed during filling at the pressure sensor locations. Also, as expected, a cure gradient was observed along the length of the part. The resin close to the vent port, which entered in the mould earliest, started curing first, followed by the resin which came after, as confirmed by experiments in Fig. 5. Resin pressure variation modeling is very important for the class A RTM processing. A pressure increase in the later stages of resin cure predicts a good contact between the composite and the mould which ultimately helps in getting good surface finish on RTM moulded parts by reproducing the mould's finish. A close match was found for the pressure variations observed during the curing of low profile polyester resins with 0%, 5%, 10% and 40% LPA. Simulations of pressure variations were also seen to be very sensitive to the parameters of the resin shrinkage–expansion model. Overall, RTM simulations were found to be very useful and quite accurate in predicting mould pre-heating, filling, curing and pressure variation behaviour of a low profile polyester resin.

Acknowledgements

The Auto21 Network of Centers of Excellence and Ecole Polytechnique de Montreal are gratefully acknowledged for their financial and technical support. We would also like to thank Dr. Michael Debolt from Ford Motors for his technical advice and support during this research. Help from Eric St-Amant of McGill Composite Materials and Structures Laboratory is gratefully appreciated.

References

[1] Martin GQ, Son JS. Fluid mechanics of mold filling for fiber reinforced plastics. In: Advanced Composites: the latest developments, proceedings of the ASM/ESD second conference on advanced composites; 1986.
[2] Friedrichs B, Guceri SI. A hybrid numerical technique to model 3-D flow fields in resin transfer molding processes. Polym Eng Sci 1995;35(23):1834–51.
[3] Friedrichs B, Guceri SI, Subbiah S, Altan MC. Simulation and analysis of mold filling processes with polymer–fiber composites. In: Tseng AA, Soh SK, editors. Proceedings of polymers and polymeric composites. ASME; 1990.

[4] Dessenberger RB, Tucker III CL. Thermal dispersion in resin transfer molding. Polym Compos 1995;16(6):495–506.
[5] Advani SG, Bruschke MV. A finite element/control volume approach to mold filling in anisotropic porous media. Polym Compos 1990;11(6):398–405.
[6] Shojaei A, Ghaffarian SR, Karimian SMH. Numerical modeling of three-dimensional mold filling process in resin transfer molding using quasi steady state and partial saturation formulations. Compos Sci Technol 2002;62(2):861–9.
[7] Lekakou C, Bader MG. Mathematical modeling of macro and micro infiltration in resin transfer molding. Composites Part A 1998;29(1–2):29–37.
[8] Young WB, Han K, Fong LH, Lee LJ. Flow simulation in molds with pre-placed fiber mats. Polym Compos 1991;12(6):391–403.
[9] Boccard A, Lee II W, Springer GS. Model for determining the vent locations and the fill time for resin transfer molds. J Compos Mater 1995;29(3):306–33.
[10] Young WB. J Compos Mater 1994;28.
[11] Young WB. Three-dimensional non-isothermal mold filling simulations in resin transfer molding. Polym Compos 1994;15(2):118–27.
[12] Trochu F, Gauvin R, Gao DM. Numerical simulation of the resin transfer molding process by the finite element method. Adv Polym Tech 1993;12(4):329–42.
[13] Gauvin R, Trochu F. Key issues in numerical simulation for liquid composite molding processes. Polym Compos 1998;19(3):233–40.
[14] Gauvin R, Trochu F, Lemenn Y, Diallo L. Permeability measurement and flow simulation through fiber reinforcement. Polym Compos 1996;17(1):34–42.
[15] Hammami A, Gauvin R, Trochu F. Modeling the edge effect in liquid composite molding. Composites Part A 1998;29(5–6):603–10.
[16] Lin RJ, Lee LJ, Liou ML. Mold filling and curing modeling of RTM and SRIM processes. In: Proceedings of 7th annual ASM/ESD advanced composite materials: new developments and applications; 1991.
[17] Antonelli D, Farina A. Resin transfer moulding: mathematical modeling and numerical simulations. Composites Part A 1999;30(12):1367–85.
[18] Shojaei A, Ghaffarian SR, Karimian SMH. Modeling and simulation approaches in the resin transfer molding process: a review. Polym Compos 2003;24(4):525–44.
[19] Haider M, Hubert P, Lessard L. Cure shrinkage characterization and modeling of a polyester resin containing low profile additives. Composites Part A 2007;38(3):994–1009.
[20] Haider M, Hubert P, Lessard L. An experimental investigation for class A surface finish in resin transfer moulding process. Compos Sci Technol 2007;67(15–16):3176–86.
[21] Rudd CD, Long AC, Kendall KN, Mangin C. Liquid moulding technologies: Resin transfer moulding, structural reaction injection moulding and related processing technologies. Woodhead Publishing Limited; 1997.
[22] Ruiz E, Trochu F. Thermo-mechanical properties during cure of glass–polyester RTM composites: elastic and viscoelastic modeling. J Compos Mater 2005;39(10):881–916.